Supplementary Information for the article "**In pancreatic islets from type 2 diabetes patients, the dampened circadian oscillators lead to reduced insulin and glucagon exocytosis"**

Authors: Volodymyr Petrenko[1,2,3,4], Nikhil R. Gandasi[5,7], Daniel Sage[6], Anders Tengholm[5], Sebastian Barg[5], and Charna Dibner[1,2,3,4]*

*Corresponding author: Dr. Charna Dibner
Division of Endocrinology, Diabetes and Nutrition, Department of Medicine
Department of Cell Physiology and Metabolism
Faculty of Medicine, University of Geneva
D05.2147c Rue Michel-Servet, 1
CH-1211 Geneva 4, Switzerland
Tel: +41 22 3795934
Email: charna.dibner@hcuge.ch

This PDF file includes:

Supplementary methods
Tables S1 to S3
Legends for Figures S1 to S5
Legends for Movies S1 to S2
SI References
Figures S1 to S5

Additional supplementary materials for this manuscript include the following:

Movies S1 to S2

Supplementary Methods

Animal care, mouse strain and pancreatic islet preparations

Animal studies were performed according to the regulations of the veterinary office of the State of Geneva (authorization number GE/159/15). Bmal1 knockout mice (Bmal1-/-) have been established by the Weitz group (Harvard) (1), and previously used by others and us as described in (2, 3). All the experiments were done in mice aged between 7 and 16 weeks, both males and females, under standard animal housing conditions with free access to food and water and in 12 h light/12 h dark cycles (LD). Heterozygous littermates were used as a control (Bmal1+/-). Islets of Langerhans were isolated by standard procedure based on collagenase (type XI; Sigma) digestion of the pancreas followed by Ficoll purification (3-5).

Quantitative Polymerase Chain Reaction (qPCR)

Total RNA was prepared from cultured islet cells using RNeasy® Plus Micro Kit (Qiagen). The RNA concentration was measured by Qubit RNA SH kit (Invitrogen). Then 0.2 µg of total RNA was reverse-transcribed using Superscript III (Invitrogen) and random hexamers and was PCR-amplified on a LightCycler 480 (Roche Diagnostics AG, Basel, Switzerland). Mean values for each sample were calculated from technical duplicates of each quantitative RT-PCR (qRT-PCR) analysis and normalized to the mean of housekeeping genes *hypoxanthine-guanine phosphoribosyltransferase* (*HPRT*) and *S9*. Primers used for this study are listed in Table S3.

Viral transduction and small interfering RNA transfection

To produce lentiviral particles, *Bmal1*-luciferase reporter (*Bmal1-luc*), *Per2*-luciferase reporter (*Per2-luc*), or Rat insulin promoter-GFP (RIP-GFP) lentivectors were transfected into 293T cells using the polyethylenimine method (6). Human islet cells were transduced with a multiplicity of infection MOI = 3.

For adenovirus transduction, islets attached to the Wilco dish were infected with preproglucagon promoter mCherry (Pppg-mCherry) adenovirus by 1 h exposure to a concentration of 10^5 fluorescence forming units (FFU)/islet, followed by addition 4 µM doxycycline to CMRL medium.

Dissociated adherent human islet cells were transfected twice with 50 nM small interfering RNA (siRNA) targeting *CLOCK* (*siClock*) or with the same amount of non-targeting *siControl* (Dharmacon, GE Healthcare, Little Chalfont, UK), using Lipofectamine® RNAiMAX reagent (Invitrogen, Carlsbad, CA, USA), with subsequent experiments performed 4-5 days post-transfection. The efficiency of this method has been validated by us in (7, 8). Due to the human islet material limitations, the efficiency could not be assessed in each experiment presented in this work, however based on our previous experiments the reproducibility of this procedure is high, resulting in at least 80% of inhibition of *CLOCK* transcript expression.

TIRF microscopy

Mouse cells were imaged using a custom-built lens-type total internal reflection (TIRF) microscope based on an AxioObserver Z1 with a 100x/1.45 objective (Carl Zeiss). Excitation was from two DPSS lasers at 491 and 561 nm (Cobolt, Stockholm, Sweden) passed through a cleanup filter (zet405/488/561/640x, Chroma) and controlled with an acousto-optical tunable filter (AA-Opto, France). Excitation and emission light were separated using a beamsplitter (ZT405/488/561/640rpc, Chroma). The emission light was chromatically separated onto separate areas of an EMCCD camera (Roper QuantEM 512SC) using an image splitter (Optical Insights) with a cutoff at 565 nm (565dcxr, Chroma) and emission filters (ET525/50m and 600/50m, Chroma). Scaling was 160 nm per pixel.

Cells transduced with adenoviruses were imaged for 50 s at 100 ms exposure with 561 (0.2-0.5 mW) for exocytosis experiments in β-cells. Similarly, for α-cells the exposure was 561 (0.5 mW) and 491 (0.5 mW). Single images of cells were acquired to measure the number of docked granules at 100ms exposure and 561 (0.2 mW) for β-cells and 561 (0.5 mW) and 491 (0.5 Mw) for α-cells.

TIRF microscopy image analysis

Exocytosis events were identified by eye based on the characteristic rapid loss of the granule marker fluorescence (1-2 frames) as described previously (9). Fluorescence from these events were treated with an algorithm implemented as MetaMorph journal which read the average pixel fluorescence in 1) a central circle (c) of 3 pxl (0.5 µm) diameter, 2) a surrounding annulus (a) with an outer diameter of 5 pxl (0.8 µm). Granule fluorescence ΔF, was obtained by subtracting the circle (c) with the annulus value (a) (ΔF=c-a). Note that ΔF is given as per-pixel average for the entire 0.5 µm-2 circle (Fig. 5). Granule density was calculated using a script that used the built-in 'find maxima' function in ImageJ (http://rsbweb.nih.gov/ij) for spot detection. Each experiment was repeated with cells from at least 2-3 independent preparations obtained from separate donors. Raw data supporting the Fig. 5 and Fig. S3 are deposited at http://dx.doi.org/10.17632/bwnrghvcpt.1.

Supplementary tables

Table S1. Donor characteristics

Donor no.	Sex	Age (years)	BMI (kg/m^2)	HbAc1 (%)
Non-diabetic donors				
1[1]	F	40	24.5	NA
2[1]	M	53	27.8	NA
3[1]	M	49	18.6	NA
4[2]	M	37	25.4	5.50%
5[1]	M	60	24.2	NA
6[2]	F	56	33.5	5.20%
7[1]	M	47	23.4	NA
8[1]	F	34	20	NA
9[2]	M	23	24.8	5.30%
10[1]	M	56	22.5	NA
11[1]	M	19	20	NA
12[1]	M	54	28.5	NA
13[3]	F	76	19.3	NA
14[4]	M	51	NA	NA
15[1]	F	59	23.7	NA
16[1]	F	41	22.4	NA
17[1]	F	51	44.1	NA
18[1]	F	47	33.4	NA
19[1]	M	49	26.2	NA
20[2]	F	48	21.5	5.30%
21[2]	M	54	22.3	5.80%
22[2]	F	46	19	5.80%

23[2]	M	66	27	4.70%
24[2]	M	25	27.3	5.20%
25[2]	F	53	22.7	4.80%
26[3]	M	23	24	5%
27[3]	F	50	31.2	5.8%
Total=27	M=15, F=12	47±13[a]	25.28±5.47[a]	5.31±0.37%[a]
Type 2 diabetic donors				
1[2]	F	55	29.8	7.40%
2[2]	M	42	43.7	6.60%
3[2]	M	51	35.6	7.10%
4[2]	M	59	27.7	6.50%
5[3]	M	51	35.3	8.60%
6[3]	M	65	21.8	9.90%
7[2]	F	48	30.4	7.50%
8[2]	M	55	29.9	8.50%
9[2]	M	63	22	7.30%
10[3]	F	54	24.4	7.20%
11[2]	M	61	27.4	7.10%
12[2]	F	37	39.3	NA
13[2]	F	37	33	13.10%
14[2]	M	53	30.1	7.80%
15[3]	M	43	25.4	6.50%
Total=15	M=10, F=5	53±8[a]	30.6±6.77[a]	7.94±1.75%[a]

M, male sex; F, female sex.
[1]Donors provided by Islet Transplantation Center of Geneva University Hospital (Geneva, Switzerland);
[2]Donors provided by Prodo Laboratories LTD company (California, US);
[3]Donors provided by Alberta Diabetes Institute islet core center (Alberta, Canada);
[4]Donors provided by Pancreatic Tissue Bank of Hospital Universitari de Bellvitge (Barcelona, Spain);
[a]Data are means ± SD.

Table S2. Circadian characteristics of *Bmal1-luc* profiles recorded from pancreatic islets derived from non-diabetic and T2D donors synchronized with the pulses of forskolin, Liraglutide, adrenaline, or Octreotide (respective data are presented in Figure 1)

Synchronizer	Islets from non-diabetic (control) donors				Islets from T2D donors			
	n	Period, h (mean ± SEM)	Phase, h (mean ± SEM)	Amplitude, counts/min (mean ± SEM)	n	Period, h (mean ± SEM)	Phase, h (mean ± SEM)	Amplitude, counts/min (mean ± SEM)
Forskolin	19	25.41 ± 0.26	8.68 ± 0.93	0.107 ± 0.013	15	25.54 ± 0.56	10.81± 0.79	0.066 ± 0.007*
Liraglutide	6	24.6 ± 0.48	12.00 ± 1.58	0.043 ± 0.006[#]	4	24.23 ± 1.25	13.5 ± 2.38	0.052 ± 0.004
Adrenaline	7	21.25 ± 0.33 [#]	6.67 ± 1.68	0.047 ± 0.007[#]	3	23.2 ± 2.3	13.6 ± 1.7	0.032 ± 0.003

Octreotide	7	24.8 ± 0.87	7.74 ± 1.6	0.063 ± 0.009	8	25.34 ± 1.06	12.02 ± 2.3	0.03 ± 0.006**,#

Parameters were calculated by CosinorJ software (10) through an automated application of optimal cosine fit to 20 min resolution recordings, based on detrended bioluminescence values (3);
n represents number of donors;
#$p < 0.05$, Student's t-test (as compared to forskolin - synchronized group);
*$p < 0.05$, **$p < 0.01$, Student's t-test (as compared to the homological groups in non-diabetic donors).

Table S3. Sequences of quantitative RT-PCR primers

Target gene		*Sequence primers*
PER1	*forward*	5'-CCCTTTGGTGACCCCAATG-3'
	reverse	5'-GCCCCATAAGGATAGCTGGAT-3'
PER2	*forward*	5'-CGCAGGGTGCGCTCGTTTGAA-3'
	reverse	5'-GCTGGGCTCTGGAACGAAGCTTTCG-3'
BMAL1	*forward*	5'-CCCTTGGACCAAGGAAGTAGAA-3'
	reverse	5'-CTTCCAGGACGTTGGCTAAAAC-3'
CRY1	*forward*	5'-GAGAACAGATCCCAATGGAGACTATAT-3'
	reverse	5'-CCTCTTAGGACAGGCAAATAACG-3'
REV-ERBα	*forward*	5'-GATCGTGAGTCGCGGGGTCC-3'
	reverse	5'-TGTAGGTGATGACGCCACCTGTGT-3'
PER3	*forward*	5'-CCTGGACCCTGAACATGCA-3'
	reverse	5'-TGTGAGCCCCACGTGTTTAA-3'
DBP	*forward*	5'-TAGAAGGAGCGCCTTGAGTC-3'
	reverse	5'-GCAACCCTCCAGTATCCAGA-3'
CLOCK	*forward*	5'-CCAGCCACCGCAACAATT-3'
	reverse	5'-GGATTCCCATGGAGCAACCTA-3'
S9	*forward*	5'-CTCCGGAACAAACGTGAGGT-3'
	reverse	5'-TCCAGCTTCATCTTGCCCTC-3'
HPRT	*forward*	5'-GATTTTATCAGACTGAGGAGC-3'
	reverse	5'-TCCAGTTAAAGTTGAGAGATC-3'
CRY2	*forward*	5'-ACTGCCCTGTGGGCTTTG -3'
	reverse	5'-TGACATCCGGTTCGTCTACA -3'

NFIL3	*forward*	5’-GGAGAAGACGAGCAACAGGT -3’
	reverse	5’-CTTTGATCTGCATGGCTTTG -3’
RORA	*forward*	5’-CTTCTTTCCCTACTGTTCGTTC -3’
	reverse	5’-GCTCTTCTCTCAAGTATTGGC -3’
REV-ERBβ	*forward*	5’-TCATGCTTGCGAAGGCTGTAA-3’
	reverse	5’-CGCTTAGGAATACGACCAAAC -3’
INS	*forward*	5’-GCAGCCTTTGTGAACCAACA-3’
	reverse	5’-CGTTCCCCGGACACTAGGTA-3’
GCG	*forward*	5’-CTGGTGAATGTGCCCTGTGA -3’
	reverse	5’-CAGGCAGACCCACTCAGTGA-3’
MAFA	*forward*	5’-CATTCTGGAGAGCGAGAAGTG-3’
	reverse	5’-TTTCTCCTTGTACAGGTCCCG-3’
GLUT1	*forward*	5’-CCATTGGCTCCGGTATCGT-3’
	reverse	5’-GCTCGCTCCACCACAAACA-3’
GLUT2	*forward*	5’-TTCCAGTACATTGCGGACTTC-3’
	reverse	5’-ACTTTCCTTTGGTTTCGTGAAC-3’
SSTR2	*forward*	5’-ATGCCAAGATGAAGACCATCAC-3’
	reverse	5’-TGAACTGATTGATGCCATCCA-3’
SLC30A8	*forward*	5’-TGGCCACAATCACAAGGAAGT-3’
	reverse	5’-CAAGGGCATGCACAAAAGC-3’
STX1A	*forward*	5’- TTAAAGAGCATCGAGCAGTCC-3’
	reverse	5’-CGACATGACCTCCACAAACTC-3’
SNAP25	*forward*	5’-ATCGGGAACCTCCGTCAC-3’
	reverse	5’-AATTCTGGTTTTGTTGGAATCAG-3’
VAMP2	*forward*	5’-GTGGACATCATGAGGGTGAA -3’
	reverse	5’-GTATTTGCGCTTGAGCTTGG-3’
ATP1A1	*forward*	5’-GGTCCCAACGCCCTCACTC-3’
	reverse	5’-ACCACACCCAGGTACAGATTATCG-3’
ADRA2A	*forward*	5’-CTGCGTTTCCTCGTCTGG-3’
	reverse	5’-CAGCAAGAAGCTTCCCTTGT-3’

Legends for supplementary figures

Figure S1. Alterations in molecular clocks and functional genes in human T2D pancreatic islets. (A) Altered mRNA expression of core-clock genes in non-synchronized human T2D islet cells. The expression levels of *CLOCK* (n = 16 ND; n = 15 T2D donors); *BMAL1* (n = 15 ND; n = 14 T2D donors); *PER1*, *PER2*, *PER3*, *CRY1* (n = 13 ND and T2D donors); *DBP* (n = 11 ND; n = 12 T2D donors); *REV-ERBα* (n = 14 ND and T2D donors); *RORA* (n = 9 ND and T2D donors); *REV-ERBβ* (n = 6 ND and T2D donors); *NFIL3* (n = 8 ND; n = 7 T2D donors); and *CRY2* (n = 13 ND; n = 9 T2D donors) transcripts. (B) Altered mRNA expression of islet functional genes in non-synchronized human T2D islet cells. The expression levels of *INS* and *GCG* (n = 8 ND; n = 6 T2D donors); *MAFA, SLC30A8* and *ATP1A1* (n = 7 ND; n = 6 T2D donors); *STX1A*, *SNAP25*, *VAMP2*, *GLUT1*, *GLUT2*, *SSTR2* and *ADRA2A2* (n = 6 ND and T2D donors). (C-D) Average raw oscillatory profiles of forskolin-synchronized ND and T2D human islets transduced with *Bmal1-luc* (C), or *Per2-luc* (D) lentiviral reporters. (E) Medium change fails to synchronize *Bmal1-luc* oscillations in human islet cells *in vitro*. Data are presented as the average detrended values of independent recordings from n = 4 ND donors. Correlations between T2D donors HbA1c and circadian amplitude (F), period length (G), and phase (H), assessed with CosinorJ software on detrended *Per2-luc* bioluminescence recordings between 20 h and 90 h (n = 14 donors).

Figure S2. Around-the-clock assessment of insulin, glucagon and proinsulin secretion in cultured primary human islets cells. (A) Fluorescence images of dispersed islet cell cultures derived from ND and T2D donors, immunostained for insulin (green labeling) and glucagon (red labeling). Cell nuclei are stained with Hoechst dye (blue labeling). (B) Histograms depicting quantification of insulin-positive β- and glucagon-positive α-cells from all plated islet cells (%, middle panel), and the percentage of β cells from all quantified α and β cells within cultures (left panel). The density of cells in cultures derived from ND and from T2D donors is shown on the right panel. (C) Total insulin (left panel), glucagon (middle panel) and proinsulin (right panel) content at the end of perifusion experiments. Concentration of insulin (D), glucagon (E) and proinsulin (F) secretion in the perifusion experiments (Fig. 4A, C, E), normalized to the RNA concentration in the dishes cultured in parallel to the perifusion experiments. All data are expressed as mean ± SEM. Two-way ANOVA test with Bonferroni post-test was used to assess the difference between experimental groups. *$p < 0.05$; **$p < 0.01$, and ***$p < 0.001$.

Figure S3. **Insulin and glucagon granule docking and exocytosis in α- and β-cells of Bmal1 KO mice.** β- (A-C) and α-cells (D-F) from WT and Bmal1KO mice. Density of docked granules (B and E) and sum of the exocytotic events (C and F) respectively are shown. Scale bar, 1 μm.

Figure S4. Impact of high glucose on the circadian clocks operative in T2D islets. Average raw oscillatory profiles of forskolin-synchronized ND (A) and T2D (B) human islets transduced with *Bmal1-luc* (left panels), or *Per2-luc* (right panels) lentiviral reporters, and recorded in presence either 5.5 mM or 20 mM glucose. Assessment of insulin secretion in forskolin-synchronized mixed islet cells from ND (C) and T2D (D) donors, perifused with the medium containing either 5.5 mM or 20 mM glucose, and collected every 4 h during 48 h. Data expresses the absolute (left panels) and detrended values (middle panels), complimentary to Figure 6C. Representative examples of *Per2-luc* bioluminescence profiles, simultaneously recorded during perifusion are shown in the right panels. (E) Apoptosis was assessed with Cell Death Detection ELISA kit on the whole islets from ND and T2D donors, previously transduced with leniviral reporters, in the end of 5-day bioluminescence recording period in presence of 5.5 mM or 20 mM

glucose. Data are expressed as absolute difference in the absorbance at wavelength A_{450} and A_{409}, mean ± SEM for n = 3 ND and n = 3 T2D donors. (F) Comparison of total insulin content in 7 h release experiments presented in Figure 6D and Figures 7C, F. Data are expressed as mean ± SEM, paired Student's t-test was used to compare different conditions within the same donor (5.5 mM glucose, 20 mM glucose and 5.5 mM glucose + Nobiletin), and unpaired Student's t-test was used to compare difference between ND and T2D islet cells incubated at 5.5 mM glucose. *$p < 0.05$, **$p < 0.01$.

Figure S5. Impact of ROR agonist Nobiletin and REV-ERB agonist SR9011 on circadian rhythm in human pancreatic islet cells. (A-B) Average bioluminescence recordings of *Per2-luc* reporter in T2D (A), and in ND donor islets (B) in the presence of Nobiletin (n = 2 for ND and T2D donors). (C) Addition of Nobiletin (arrow) boosts expression of *Bmal1-luc* reporter in T2D islet cells, previously synchronized with forskolin. (D) Assessment of apoptosis in ND and T2D islets treated with Nobiletin during continuous bioluminescence recordings for 5 days. The apoptosis measurement was conducted in the end of bioluminescence experiment for n = 3 ND and n = 3 T2D donors. (E-F) Nobiletin does not influence insulin content in human islet cells. (E) Total amount of insulin produced during 7 h in release experiments (Fig. 7C, F; secreted insulin plus residual insulin content) in the presence and absence of Nobiletin in the culture medium. Data are expressed as mean ± SEM. Paired Student's t-test, n = 4 ND and n = 5 T2D donors. (F) Total amount of insulin measured during GSIS experiments. Total amount was calculated as a sum of insulin secreted at 2.8 mM, 16.7 mM and repeated 2.8 mM plus insulin residual content in the presence or absence of Nobiletin in the medium (Fig. 7D, G). Data are expressed as mean ± SEM. Paired Student's t-test, n = 4 ND and n = 4 T2D donors. (G) Nobiletin stimulates glucagon release by human islet cells in 7 h release experiments (n = 3 ND donors, and n = 3 T2D donors). Data are expressed as mean ± SEM, Student's t-test. (H) REV-ERBs agonist SR9011 diminishes *Per2-luc* expression. Average bioluminescence recordings of *Per2-luc* reporter in ND donor islets in the presence of SR9011, n = 2 donors.

Legends for supplementary movies

Movie S1. Combined bioluminescence-fluorescence time-lapse microscopy of human pancreatic islets from ND donors. Human α- and β-cells were labeled with adenovirus carrying Pppg-mCherry construct (red labeling) or with RIP-GFP lentiviruses (green) respectively, and with the *Per2-luc* bioluminescence reporter (blue) (see also Fig. 2A-B). Bioluminescence signal was measured over α- and β-cells within the area encircled in yellow. Representative trajectories are traced in the colors of rainbow over the image, illustrating the movement of the traced cell between the first time-lapse image traced in red, through the entire set of images acquired every hour until the last image traced in blue. Islets were synchronized by a 1 h forskolin pulse (time point 0), and subsequently subjected to bioluminescence-fluorescence time-lapse microscopy for at least 70 h. Upper left video shows bioluminescence acquisition; upper right video is a merge of bioluminescence channel (blue), green fluorescence channel (RIP-GFP expression), and red fluorescence channel (Pppg-mCherry expression). Lower videos represent a close-up of one islet from the corresponding upper videos (the enlarged area is indicated with the blue square on the video).

Movie S2. Combined bioluminescence-fluorescence time-lapse microscopy of human pancreatic islets from T2D donors. Human α- and β-cells within islets from T2D donors were labeled, imaged and analyzed as described in the legend to Movie S1. Islets were synchronized by a 1 h forskolin pulse (time point 0), and subsequently subjected to bioluminescence-fluorescence

time-lapse microscopy for at least 70 h. Upper left video shows bioluminescence acquisition; upper right video is a merge of bioluminescence channel (blue), green fluorescence channel (RIP-GFP expression), and red fluorescence channel (Pppg-mCherry expression). Lower videos represent a close-up of one islet from the corresponding upper videos (the enlarged area is indicated with the blue square on the video).

References

1. K. F. Storch *et al.*, Intrinsic circadian clock of the mammalian retina: importance for retinal processing of visual information. *Cell* **130**, 730-741 (2007).
2. C. Jouffe *et al.*, The circadian clock coordinates ribosome biogenesis. *PLoS Biol* **11**, e1001455 (2013).
3. V. Petrenko *et al.*, Pancreatic alpha- and beta-cellular clocks have distinct molecular properties and impact on islet hormone secretion and gene expression. *Genes & development* **31**, 383-398 (2017).
4. V. Petrenko, Y. Gosmain, C. Dibner, High-Resolution Recording of the Circadian Oscillator in Primary Mouse alpha- and beta-Cell Culture. *Front Endocrinol (Lausanne)* **8**, 68 (2017).
5. V. Petrenko, C. Dibner, Cell-specific resetting of mouse islet cellular clocks by glucagon, glucagon-like peptide 1 and somatostatin. *Acta Physiol (Oxf)* **222**, e13021 (2018).
6. P. Pulimeno *et al.*, Autonomous and self-sustained circadian oscillators displayed in human islet cells. *Diabetologia* **56**, 497-507 (2013).
7. C. Saini *et al.*, A functional circadian clock is required for proper insulin secretion by human pancreatic islet cells. *Diabetes, obesity & metabolism* **18**, 355-365 (2016).
8. V. Petrenko, C. Saini, L. Perrin, C. Dibner, Parallel Measurement of Circadian Clock Gene Expression and Hormone Secretion in Human Primary Cell Cultures. *J Vis Exp* 10.3791/54673 (2016).
9. N. R. Gandasi *et al.*, Glucose-Dependent Granule Docking Limits Insulin Secretion and Is Decreased in Human Type 2 Diabetes. *Cell Metab* **27**, 470-478 e474 (2018).
10. T. Mannic *et al.*, Circadian clock characteristics are altered in human thyroid malignant nodules. *J Clin Endocrinol Metab* **98**, 4446-4456 (2013).

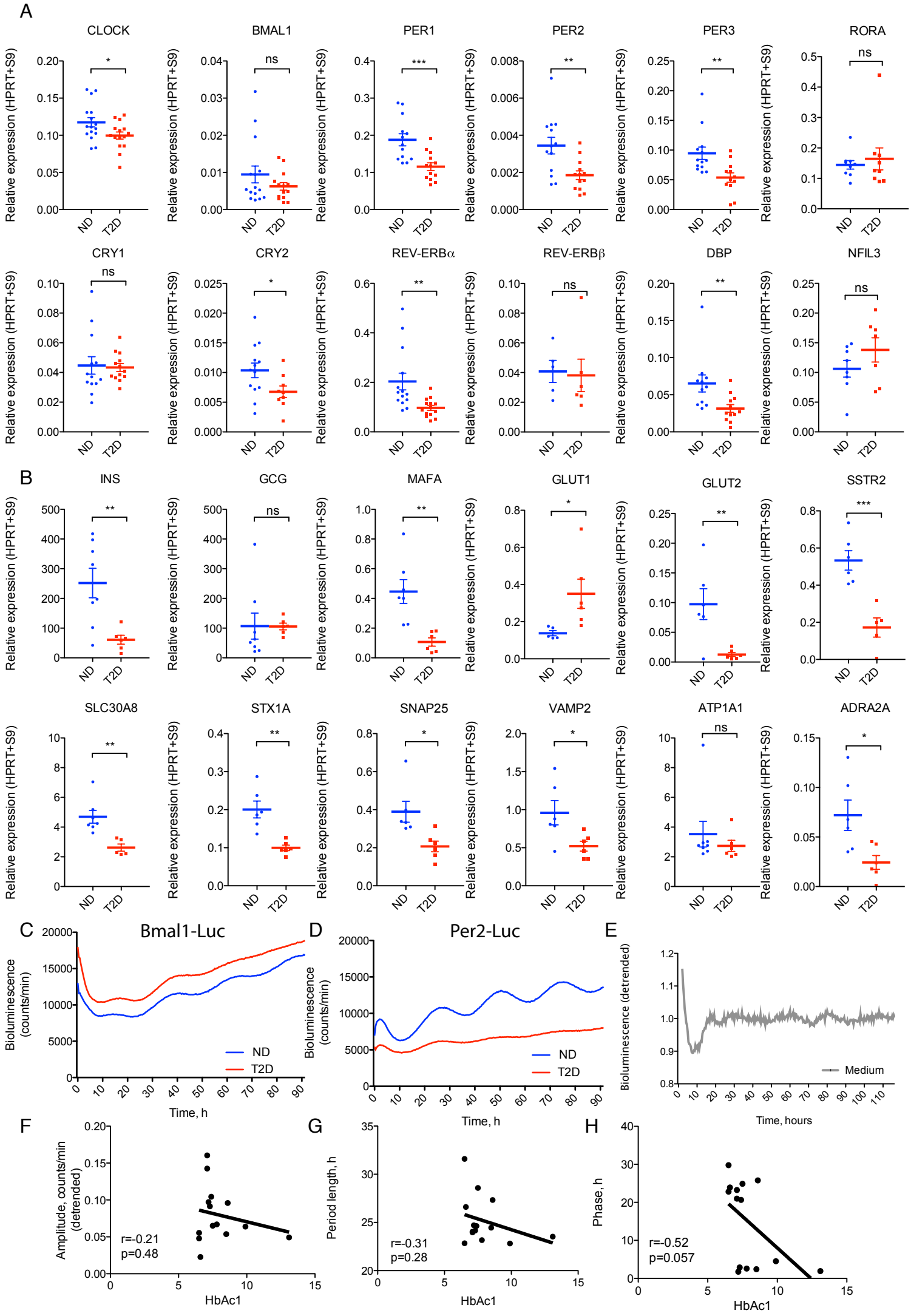
A
CLOCK
BMAL1
PER1
PER2
PER3
RORA
CRY1
CRY2
REV-ERBα
REV-ERBβ
DBP
NFIL3
B
INS
GCG
MAFA
GLUT1
GLUT2
SSTR2
SLC30A8
STX1A
SNAP25
VAMP2
ATP1A1
ADRA2A
Relative expression (HPRT+S9)
ND
T2D
C
Bmal1-Luc
Bioluminescence (counts/min)
Time, h
D
Per2-Luc
E
Bioluminescence (detrended)
Medium
Time, hours
F
Amplitude, counts/min (detrended)
r=-0.21
p=0.48
HbAc1
G
Period length, h
r=-0.31
p=0.28
H
Phase, h
r=-0.52
p=0.057

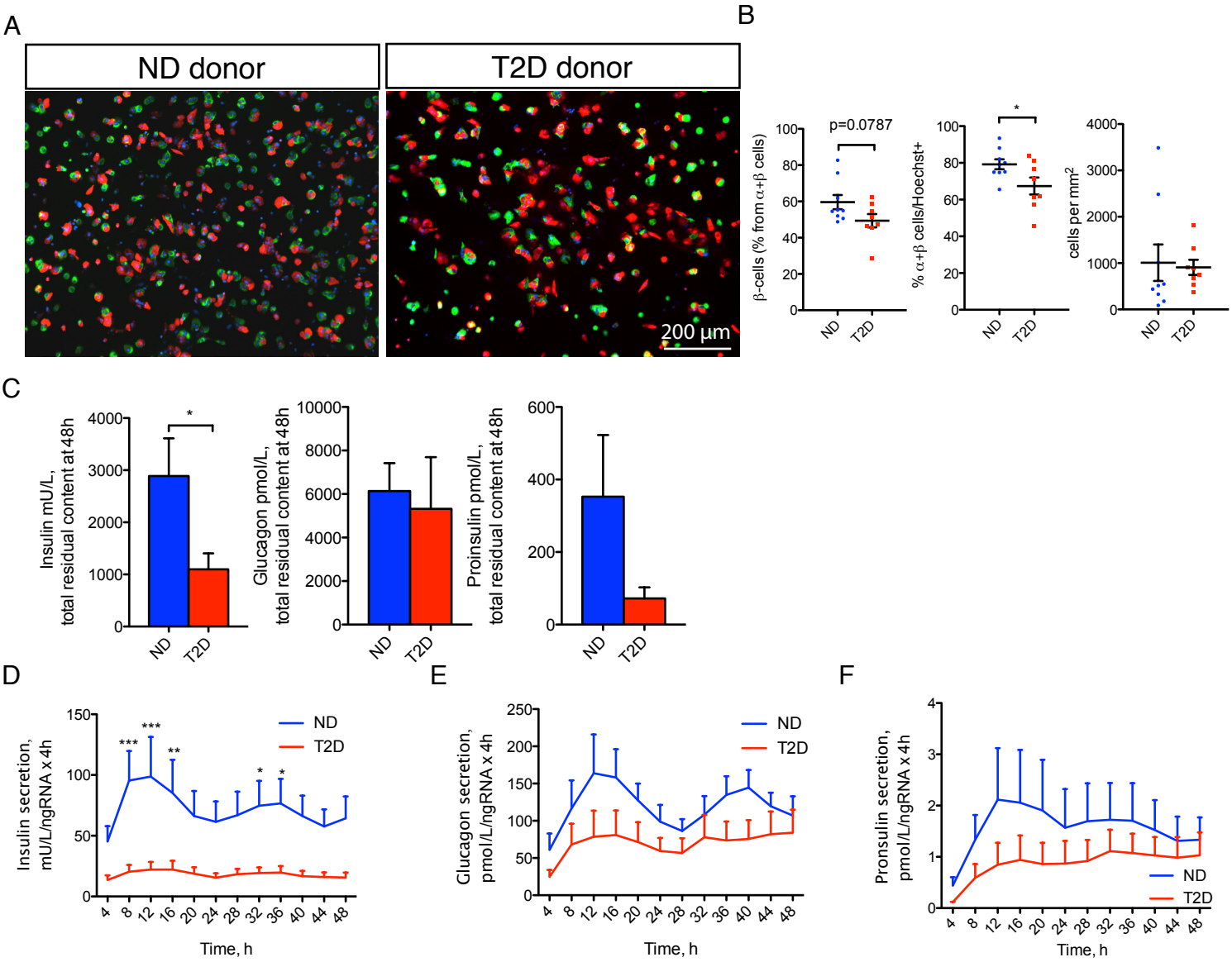
A
ND donor
T2D donor
200 µm
B
β-cells (% from α+β cells)
p=0.0787
% α+β cells/Hoechst+
cells per mm2
ND
T2D
C
Insulin mU/L, total residual content at 48h
Glucagon pmol/L, total residual content at 48h
Proinsulin pmol/L, total residual content at 48h
D
Insulin secretion, mU/L/ngRNA x 4h
E
Glucagon secretion, pmol/L/ngRNA x 4h
F
Pronsulin secretion, pmol/L/ngRNA x 4h
Time, h

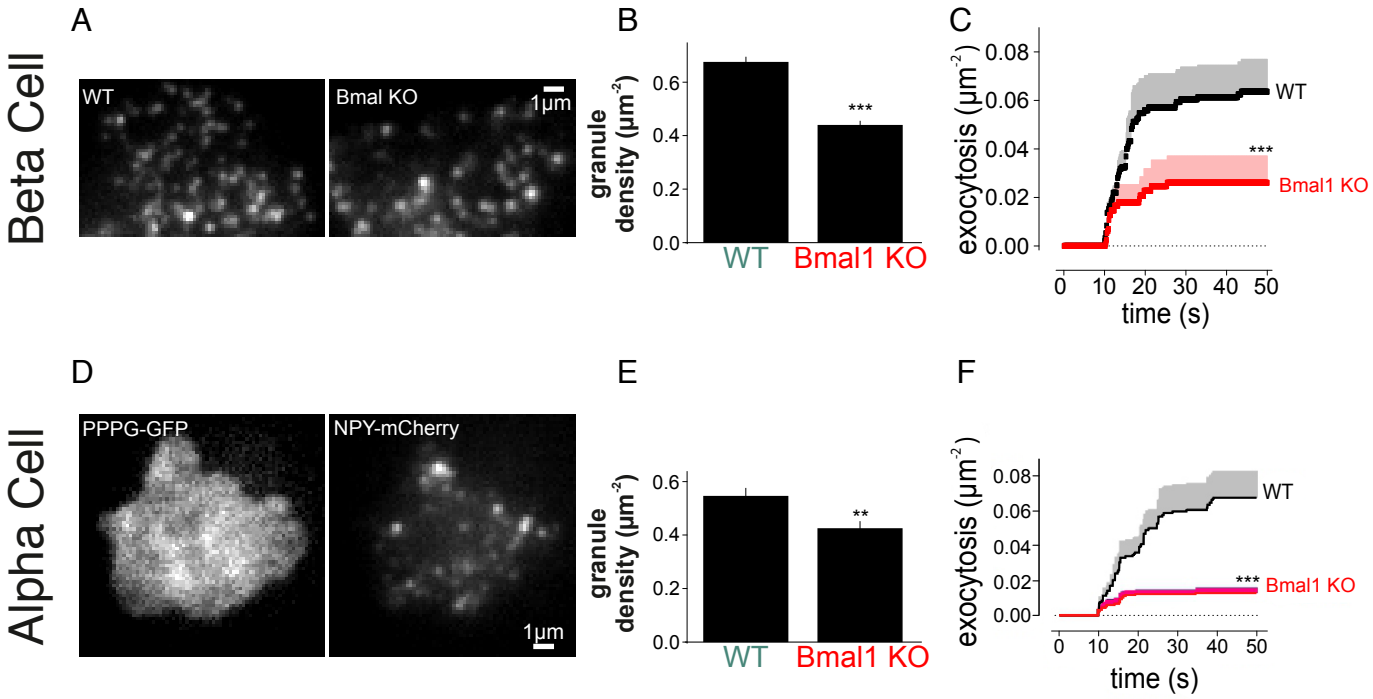
Beta Cell
A
WT
Bmal KO
1µm
B
granule density (µm-2)
0.6
0.4
0.2
0.0
***
WT
Bmal1 KO
C
exocytosis (µm-2)
0.08
0.06
0.04
0.02
0.00
WT
***
Bmal1 KO
0 10 20 30 40 50
time (s)
Alpha Cell
D
PPPG-GFP
NPY-mCherry
1µm
E
granule density (µm-2)
0.6
0.4
0.2
0.0
**
WT
Bmal1 KO
F
exocytosis (µm-2)
0.08
0.06
0.04
0.02
0.00
WT
***
Bmal1 KO
0 10 20 30 40 50
time (s)

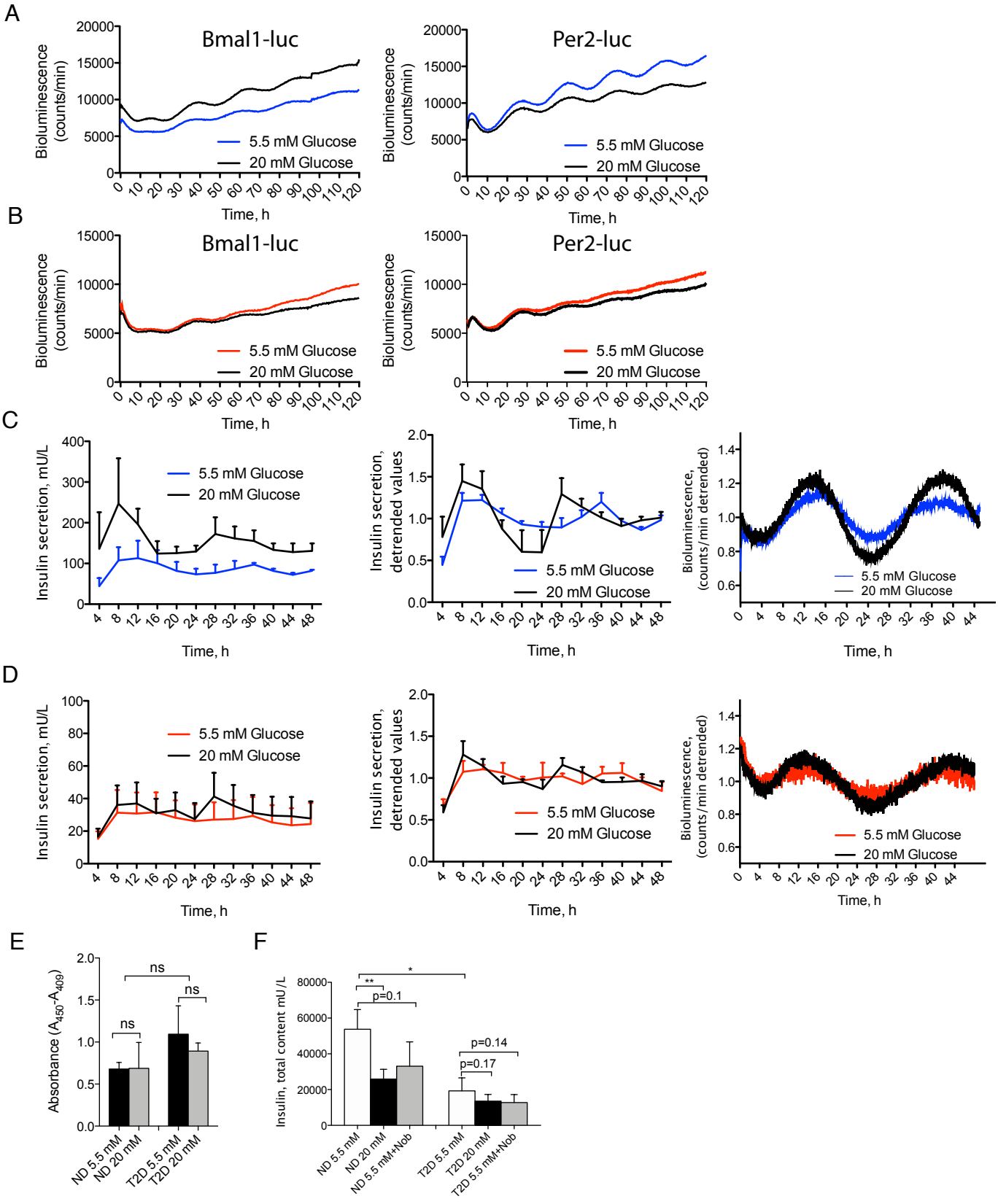
A
Bmal1-luc
Per2-luc
Bioluminescence (counts/min)
5.5 mM Glucose
20 mM Glucose
Time, h
B
Bmal1-luc
Per2-luc
Bioluminescence (counts/min)
5.5 mM Glucose
20 mM Glucose
Time, h
C
Insulin secretion, mU/L
Insulin secretion, detrended values
Bioluminescence, (counts/min detrended)
5.5 mM Glucose
20 mM Glucose
Time, h
D
Insulin secretion, mU/L
Insulin secretion, detrended values
Bioluminescence, (counts/min detrended)
5.5 mM Glucose
20 mM Glucose
Time, h
E
Absorbance (A450-A409)
ns
ns
ns
ND 5.5 mM
ND 20 mM
T2D 5.5 mM
T2D 20 mM
F
Insulin, total content mU/L
*
**
p=0.1
p=0.14
p=0.17
ND 5.5 mM
ND 20 mM
ND 5.5 mM+Nob
T2D 5.5 mM
T2D 20 mM
T2D 5.5 mM+Nob

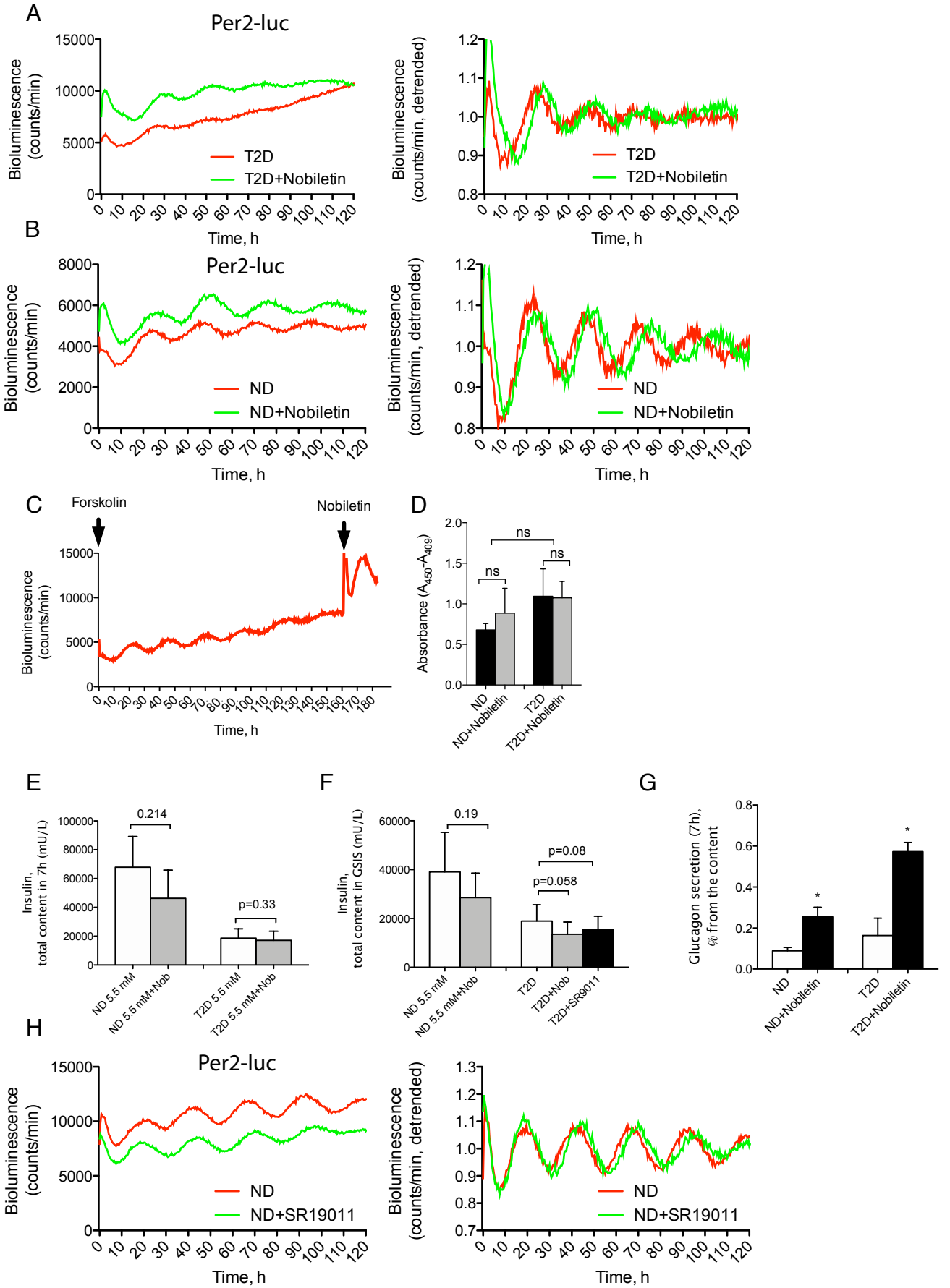
A
Per2-luc
Bioluminescence (counts/min)
T2D
T2D+Nobiletin
Time, h
Bioluminescence (counts/min, detrended)
B
ND
ND+Nobiletin
C
Forskolin
Nobiletin
D
Absorbance (A450-A409)
ns
E
Insulin, total content in 7h (mU/L)
0.214
p=0.33
ND 5.5 mM
ND 5.5 mM+Nob
T2D 5.5 mM
T2D 5.5 mM+Nob
F
Insulin, total content in GSIS (mU/L)
0.19
p=0.08
p=0.058
T2D
T2D+Nob
T2D+SR9011
G
Glucagon secretion (7h), % from the content
ND
ND+Nobiletin
T2D
T2D+Nobiletin
H
ND+SR19011